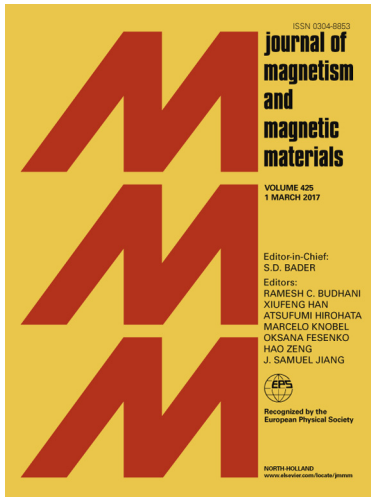

Effect of Oxygen Partial Pressure on the Density of Antiphase Boundaries in Fe_3O_4 Thin Films on Si(100)

Suraj Kumar Singh, Sajid Husain, Ankit Kumar, Sujeet Chaudhary

PII: S0304-8853(17)30471-7
DOI: http://dx.doi.org/10.1016/j.jmmm.2017.07.082
Reference: MAGMA 63013

To appear in: *Journal of Magnetism and Magnetic Materials*

Received Date: 10 February 2017
Revised Date: 14 July 2017
Accepted Date: 21 July 2017

Please cite this article as: S.K. Singh, S. Husain, A. Kumar, S. Chaudhary, Effect of Oxygen Partial Pressure on the Density of Antiphase Boundaries in Fe_3O_4 Thin Films on Si(100), *Journal of Magnetism and Magnetic Materials* (2017), doi: http://dx.doi.org/10.1016/j.jmmm.2017.07.082

Effect of Oxygen Partial Pressure on the Density of Antiphase Boundaries in Fe_3O_4 Thin Films on Si(100)

Suraj Kumar Singh[a,b†], Sajid Husain[b†], Ankit Kumar[c§], and Sujeet Chaudhary[b]*

[a]*Department of Physics, NTNU, Norwegian University of Science and Technology, N-7491 Trondheim, Norway*

[b]*Thin Film Laboratory, Department of Physics, Indian Institute of Technology Delhi, New Delhi 110016 (INDIA)*

[c]*Ångström Laboratory, Department of Engineering Sciences, Box 534, SE-751 21 Uppsala, Sweden*

Abstract:

The polycrystalline Fe_3O_4 thin films are grown on Si(100) substrate by reactive DC sputtering at different oxygen partial pressure (P_{O_2}) for controlling the growth associated density of antiphase boundaries (APBs). The micro-Raman analyses were performed to study the structural and electronic properties in these films. The growth linked changes in the APBs density are probed by electron-phonon coupling strength (λ) and isothermal magnetization measurements. The estimated values of λ are found to vary from 0.39 to 0.56 with the increase in P_{O_2} from 2.2×10^{-5} to 3.0×10^{-5} Torr, respectively. The saturation magnetization (saturation field) values are found to increase (decrease) from 394 (5.9) to 439 (3.0) emu/cm^3 (kOe) with the increase in P_{O_2}. The sharp Verwey transition (~120 K), low saturation field, high saturation magnetization and low value of λ (comparable to the bulk value ~0.51) clearly affirm the negligible amount of APBs in the high oxygen partial pressure deposited thin films.

Keywords: Fe_3O_4, anti-phase boundaries, Verwey transition

**E-mail: sujeetc@physics.iitd.ac.in* (author for correspondence)

§chainutyagi@gmail.com

† Equally contributing authors

Introduction

Magnetite (Fe_3O_4) is a cubic spinel ferrimagnetic system which shows intriguing structural, electrical and magnetic properties[1]. By virtue of its half-metallicity, 100% spin polarization, and higher Curie temperature (T_C ~ 860 K), Fe_3O_4 is a strong candidate for spintronics application such as spin valves and magnetic tunnel junctions[2][3][4][5]. However there are formation of certain defects like stacking faults at ionic sublattices during film growth are responsible for local anti-ferromagnetic ordering of the spins which leads to the formation of antiphase boundaries (APBs) which are dominantly antiferromagnetic coupled between adjacent domains in Fe_3O_4 thin films [6][7]. The APBs decrease half-metallic nature (spin polarization) and degrade electric and magnetic properties of the sputtered Fe_3O_4 thin films. The formation of APBs results in the reduction of saturation magnetization, delay in saturation field, increase in resistivity, broadening or disappearance of Verwey transition [8][9]. The formation of APBs in sputtered films is highly process dependent and strongly depends on growth parameters such as growth temperature, oxygen partial pressure, and nature of substrate [10][11]. The APBs form during coalescence of nuclei in the initial stage of film growth, and can be reduced at higher growth temperature since density of APBs is thermally diffusive in nature. Its perceived cause is the limited surface ad-atom mobility of growing film. Hence, to reduce APBs, it is therefore preferable to work at higher growth temperature which increases the ad-atom mobility. High growth temperature not only reduces the density of APBs but also expected to enhance the structural quality and magnetic features [9]. Thin films of Fe_3O_4 have been grown by different techniques including sputtering [12], molecular beam epitaxy [13], electron beam evaporation [14], and pulsed laser deposition on various substrates such as MgO, $MgAl_2O_4$, $SrTiO_3$, and sapphire etc[15]. There are several reports on reduction of APBs by tuning the growth temperature while preventing interfacial diffusion, and by applying the electric field during

growth [9][10][16]. In this work, we systematically investigated the effect of substrate temperature on the phase formation and impact of oxygen stoichiometry on the growth of pure phase and the density of APBs in the sputtered magnetite (Fe_3O_4) thin films. Electron-phonon coupling parameters in conjunction with isothermal magnetization measurements were used to examine the density of APBs in polycrystalline Fe_3O_4 thin films. Further, the Verwey transition (T_V) temperature using magnetization and electrical transport measurement was analysed in detail.

1. Experimental methods

The Fe_3O_4 thin films were grown by reactive pulsed DC magnetron sputtering using pure iron target (99.99%) with fixed oxygen partial pressure (P_{O_2}) of 3.0×10^{-5} Torr at different constant temperature such as 400°C, 500°C, and 600°C on Si(100) substrate to optimize the growth temperature. After the optimization of growth temperature, i.e., 500°C, the Fe_3O_4 thin films of constant thicknesses were deposited at different P_{O_2} of 2.2, 2.5, 2.8 and 3.0×10^{-5} Torr, respectively. The samples were named as F2.2, F2.5, F2.8 and F3.0, based on their P_{O_2}. The base pressure in the chamber was maintained better than 2.0×10^{-6} Torr and sputtering was done using Ar gas at a working pressure of 1.9 mTorr. The thicknesses of the films were measured using surface profilometry employing a Bruker *Dektak XT* profiler system (Billerica, MA, USA) and found to be 68nm. The X-ray diffraction (XRD) patterns were recorded using PANalytical X'Pert-Pro X-ray diffractometer in glancing angle mode at 1° using Cu K_α (1.541 Å) radiation. The phase purity of the samples was analysed by Renishaw Invia reflex micro-Raman spectrometer using air-cooled Ar-ion laser (514 nm) of 50 mW power. All Raman spectra were recorded at room temperature. Saturation magnetization and the thermo-magnetization measurements were performed by the vibrating sample magnetometer (VSM) module of the Quantum Design make Physical Property Measurement

System (QD PPMS-VSM) Evercool-II. The electrical transport (resistivity vs. temperature) measurements were performed in four probe geometry in QD PPMS using AC transport option.

2. Results and discussion

3.1 X-ray diffraction

Figure 1 shows the x-ray diffraction patterns of Fe_3O_4 thin films grown at various oxygen partial pressures (P_{O_2}) at 500°C substrate temperature. In the sample F2.2 peaks corresponding to (311) (400) and (440) crystallographic orientation were observed which indicate the polycrystalline nature of Fe_3O_4 thin films. The broadening observed in the peaks corresponding to the (400) and (440) crystallographic orientations in lowest P_{O_2} = 2.2×10^{-5} Torr grown sample indicates poor crystallinity and the possibility of partial existence of other Fe-O phase(s) [17]. On increasing P_{O_2} past 2.2×10^{-5} Torr, the (440) peak disappears in all the samples which is a signature of texture improvement. Further increasing the P_{O_2} to 2.8×10^{-5} Torr (sample F2.8) results in preferred oriented film growth with (400) crystallographic orientation whereas sample deposition at P_{O_2} = 3.0×10^{-5} Torr results in diminishing of the preferred crystallographic growth. These results clearly indicate the P_{O_2} induced changes in the crystallographic orientations of the grown thin films. Thus the crystalline quality of the films was improved on increasing the P_{O_2} under controlled way, and the optimum P_{O_2} was found to 2.8×10^{-5} Torr (F2.8) where only (400) crystallographic orientation was observed. The lattice parameters were calculated using Bragg's diffraction relation and found to vary in the range of 8.102-8.384 Å for all the samples which are comparable to the bulk value (8.396Å) of Fe_3O_4. The observed variation in the lattice parameter values have understandably resulted from the different P_{O_2} induced changes in the crystallographic orientations in the samples. The average crystallite/grain size of these films have been

calculated using the Scherrer formula [18] and is found to be ~23 nm. It is important to mention here that the estimated crystallite/grain sizes might lie in the range of the superparamagnetic (SPM) limit reported in nanoparticle samples [19]. However, the presently studied samples are thin films and the magnetization measurements (M-H and M-T) did not exhibit any signature of the SPM behaviour (which is discussed in the forthcoming section). Therefore, the possibility of grain sizes linked SPM feature in the thin film samples is ruled out. It may also here be pointed out that although the analysis of XRD peaks indicating our thin films are truly Fe_3O_4, the occurrence of γ-Fe_2O_3, however, cannot ruled out due to the fact that all Bragg diffraction peaks of Fe_3O_4 and γ-Fe_2O_3 which appears at nearly same 2ϑ positions. Therefore, to confirm the presence of Fe_3O_4 pure phase, the Raman measurements were performed on all the samples at room temperature.

3.2 Raman Analysis

This technique is highly sensitive to differentiate all the different phases of any compound such as iron oxides; Fe_3O_4 (magnetite), α-Fe_2O_3 (hematite), γ-Fe_2O_3 (maghemite), FeO (wustite) [6]. Theoretically, magnetite exhibits 14 vibrational modes ($3A_{1g} + 3E_g + 8T_{2g}$), and out of 14 modes 5 mode are Raman active at room temperature according to group theory [20]; 669cm^{-1}(A_{1g}); 410cm^{-1}(E_g); 193cm^{-1}($T_{2g}(1)$); 538cm^{-1}($T_{2g}(2)$); and 307cm^{-1} [$T_{2g}(3)$]. However, four modes(experimentally) at 668, 538, 306, and 193 cm^{-1} out of five (theoretically) predicted Raman active modes are observed at ambient conditions in non-polarized spectrum of magnetite thin films[2]. It is to be noted that the A_{1g} mode arises due to symmetric stretching of oxygen atoms along Fe-O bond which is link to the structural properties of Fe_3O_4 thin films and T_{2g} modes arise due to the symmetric and asymmetric bending of oxygen with respect to Fe ions are linked to the electronic properties of the magnetite(Fe_3O_4) thin films.

Figure 2(a) shows the Raman spectra recorded for the sample grown at different temperatures, 400°C to 600°C in step of 50°C, keeping P_{O_2} (3.0×10^{-5} Torr) fixed. It has been observed that the sample deposited at 500°C exhibit very strong A_{1g} and T_{2g} modes compared to other samples. The observed Raman spectra does not exhibit any signature of γ-Fe_2O_3 phase for which the peaks are expected to observe at 350, 500 and 700 cm^{-1}. Thus, the sputtered Fe_3O_4 thin films are of pure single phase nature. Therefore, the optimum growth temperature is 500°C for further growth of Fe_3O_4 thin films. After optimization, the Fe_3O_4 thin films were prepared at different P_{O_2} ranges from 2.2 to 3.0×10^{-5} Torr keeping 500°C growth temperature fixed. Fig 2(b) shows the Raman spectra recorded at room temperature on F2.2, F2.5, F2.8 and F3.0 samples. The increment in the intensity of A_{1g} mode with the increase in P_{O_2} indicates the improvement of the crystalline quality of Fe_3O_4 thin films. The least intensity of A_{1g} in F2.2 indicate the minimum formation of Fe_3O_4 which may show large Ms low Hc (which is discussed in the forthcoming section).

The presence of certain growth defects, like stacking faults at ionic sites, create the magnetic disorder which is known as anti-phase boundaries (APBs) in this system. These APBs cause anti-ferromagnetic (AF) couplings in polycrystalline (inter and intra grain) and epitaxial (intra grain) films by the super-exchange interactions at cationic/ionic sites. The strength of these AF interactions is found to be dependent on the angle of orientation between the two neighbouring crystallites. Since APBs are associated with magnetic disorder, therefore, the electron-phonon coupling interaction in the crystal lattice can be used to probe these boundaries indirectly. In order to estimate the density of APBs in thin films, the electron phonon coupling 'λ' has been used to evaluate using T_{2g} (3) mode line shape parameters. Figure 3(a) and 3(b) show the A_{1g} and T_{2g} Raman mode peaks respectively, fitted (red line) using Lorentzian function. The extracted line shape parameters are shown in

Table.1. Subsequently the electron-phonon coupling constant strength for the A_{1g} and T_{2g} (3) modes was evaluated using Allen's formula [6],

$$\lambda_m = \frac{g_m}{2\pi} \frac{1}{N(E_F)} \frac{\Gamma_m}{\omega^2},$$

where Γ_m is the FWHM, ω frequency is the frequency, $N(E_F)$= 3 states/eV (density of states at Fermi level) and g_m is the degeneracy of the m^{th} mode.

As P_{O_2} is increased, the peak position of A_{1g} mode can be seen to be shifted towards higher values which indicate the crystallinity improvement/variation in these thin films as the oxygen content in the plasma varied is also evident from the XRD spectra. The values of λ were obtained for T_{2g} (3) mode which varies from ~0.472 to ~0.592 for the variation of P_{O_2} from 2.2 to 3.0×10^{-5} Torr, respectively, which are comparable to the bulk value (λ = 0.51) of Fe_3O_4 [20], except F3.0 sample, though the difference is negligible, which might be due to the excessive oxygen induced surface oxidation of the grown film. We would like to emphasize that the method for estimating the density of APBs based on the electron-phonon coupling coefficient is rather indirect. However to conclude the reduction of APBs in our samples we have to look for magnetization measurements because reduction of APBs results the decrease in magnetization saturation field, decrease in magnetization, and sharpness of Verwey transition.

3.3 Magnetization (*M-H*) and Thermo-Magnetization (*M-T*) Analysis

Figure 4 shows the in-plane magnetization hysteresis (M-H) loops on the samples grown at different P_{O_2}; F2.2; F2.5; F2.8; F3.0. It is inferred from M-H measurements that the saturation fields (H_S) decreases from 5.9kOe to 3 kOe on increase the P_{O_2} from 2.2 to 3.0×10^{-5} Torr, respectively. Further, the saturation magnetization (Ms) values are found to be 663±12, 394±8, 439±9, and 422±9 emu/cc for F2.2, F2.5, F2.8, and F3.0 samples,

respectively. The observed value of M_s in F2.2 is found to be greater than the bulk value of Fe_3O_4 single crystal [9]. This enhancement in the M_s value could stem from the lower oxygen P_{O_2} induced growth of this sample compared to other films, which might result unoxidised Fe and/or formation of paramagnetic FeO phase along with Fe_3O_4 phase. Due to the presence of Fe atoms possibly either at interface and/or in the inter-granular regions, some of the exchange interactions are broken in Fe_3O_4 matrix which can result in the uncompensated magnetic moment. These uncompensated moments along with lower P_{O_2} prompted formation of traces of paramagnetic FeO phase which might be responsible for the increase in the magnetization with an increase in the applied magnetic field in F2.2 sample [21]. The significant decrease in the coercivity (H_c) value from 314 Oe to 298 Oe is also evident with the decrease in the P_{O_2}. The smallest H_c is found to be 298 Oe for F2.2 sample which is relatively low compared to the optimum value of F2.8 in perfect Fe_3O_4 phase [22]. Further, Raman spectra revealed that the intensity of structurally active A_{1g} mode peak is lowest in F2.2 sample compared to those in the other samples, a feature which is also analogous and consistent to the XRD findings (see Fig. 1). These results indirectly indicate the presence of unreacted Fe and/or paramagnetic FeO phase along with the Fe_3O_4 phase in this F2.2 sample. The early saturation field observed in higher P_{O_2} deposited samples F2.8 and F3.0 compared to F2.2 and F2.5, indicates less density of APBs in these thin films. The optimum Ms value of the sample F2.8 was found to be 439±9 emu/cc which is close to bulk value (~450 emu/cc) for Fe_3O_4 thin film [12].

The APBs prominently affects the equilibrium magnetization behaviour in these Fe_3O_4 thin films, thus, the temperature dependent magnetization (M-T) i.e., zero field cooled (ZFC) and field cooled (FC) magnetization behaviour has been examined in detail. Fig. 5 shows the ZFC and FC curves (measured at 200Oe) for all the samples grown in various P_{O_2} environments. The M-T fall in the range of 120-128K in all the sample is associated to the

metal-insulator transition in Fe_3O_4 also known as Verwey transition. The Verwey transition temperature (Tv) value for the single crystal is ~120K [8][20]. The Verway transition is accompanied by the change in crystal symmetry from cubic to rhombohedrically distorted monoclinic phase, and is very sensitive to the stoichiometry parameter and also on the density of APBs. A minute stoichiometry variations ($Fe_{3-\delta c}O_4$; δ_c ~ 0.0117) and presence of the APBs can significantly broaden/diminish the Verwey transition as reported in Ref. [11]. The broadening is attributed to the presence of ionic vacancies at octahedral sites which basically reduce the exchange interaction among the octahedral ionic sites and therefore responsible for the formation of APBs. These ionic vacancies induce strain in the lattice and result in the suppression of orthorhombic/monoclinic deformation (structural transition from cubic to orthorhombic/monoclinic) at Verwey transition. The APB induced strain not only broadens T_V but it also shifts the transition point towards lower temperature. To understand the effect of different P_{O_2} on the grown Fe_3O_4 thin films with regards to the Verwey transition temperature, the dM/dT of field cooled warming M-T profiles have been evaluated for all the samples. Figs. 6 (a)-(d) shows the change in T_V from 128 to 120 K with the increase in P_{O_2} from 2.2 to 3.0×10^{-5} Torr. It may be noted that T_V of single crystal Fe_3O_4 is 120 K [23]. However, the observed ΔT_V values of F2.2, F2.5, F2.8 are found to lie in the range of 20-25K which is comparable to the previous reported results on nearly APBs free Fe_3O_4 thin films [9]. Although, the sample F3.0 exhibit significant broadening (ΔT_V) compared to other samples suggests the presence of magnetic disorder which might be formed due to the excessive oxygen flow induced chemical disordering within the unit cell of Fe_3O_4. This is also consistence with the estimated value of λ which is higher in this F3.0 sample compared to others as shown in Table 1. Furthermore, the isotropic transition temperature (T_K) at which easy axis changes from (111) to (100) is almost similar (~130K) for all the samples.

3.5 Electrical transport (*R-T*)

Figure 7 shows the resistivity $\rho(T)$ vs. temperature behaviour for all the samples. The observed resistivity values are coinciding with the reported results on thin films having low density of APBs [11]. The Verwey transition temperature is plotted in Figs. 7(a)-(d). The significant rise in resistivity below T_V, in respective samples, exhibits metal-insulator transition. The observed values of T_V i.e., 128 K, 126 K, 126 K, and 120 K for F2.2, F2.5, F2.8, and F3.0 samples, respectively, matching with the values observed from M-T data for respective samples. The higher value of resistivity below T_V in F2.8, and F3.0 sample compared to others implies better metal-insulator transition (Verwey transition). This finding is in agreement with Raman results which exhibit the sharp intensity of A1g mode i.e., better Fe_3O_4 phase formation in F2.8 and F3.0 sample. The observed Verwey transition in our samples is comparatively sharp compared to recently reported results on polycrystalline Fe_3O_4 thin films [24][25]. Above discussion concludes that sample F2.8 and F3.0 are better quality compared to F2.2 and F2.5 samples. The low value of λ, higher value of M_S, low value of H_S, sharp value of ΔT_V, large drop in magnetization ΔM_V at Verwey transition affirm that the sample F2.8, grown at 2.8×10^{-5} Torr, exhibits reduced density of APBs.

3. Conclusions

Fe_3O_4 thin films were deposited on Si(100) substrate at different constant oxygen partial pressures ranges from 2.2 to 3.0×10^{-5} Torr at optimized growth temperature (500°C). X-ray diffraction patterns demonstrate the polycrystalline nature of all different constant oxygen partial pressures grown Fe_3O_4 thin films. The phase purity of the samples was confirmed by using Raman. X-ray diffraction and Raman spectra analysis confirm the improvement of the crystalline quality of the samples with the increase in oxygen partial pressures. The magnetization hysteresis loops, magnetization versus temperature, and resistivity versus temperature measurements in conjunction to extracted low value of electron-phonon coupling constant confirm the reduction in APBs in higher oxygen partial pressures deposited Fe_3O_4

thin films. The thermo-magnetization and electron-transport behaviour confirm the occurrence of sharp Verwey transition in all the samples.

Acknowledgments

SKS thank the ministry of HRD, Government of India, for providing the scholarship. SH acknowledges the Department of Science and Technology for providing INSPIRE fellowship. Authors thank the NRF facilities of IIT Delhi for micro-Raman measurements. We also acknowledge the Ministry of Information Technology, Government of India for providing the financial grant to carry out this work.

References:

[1] S.A. Wolf, D.D. Awschalom, R.A. Buhrman, J.M. Daughton, S. von Molnar, M.L. Roukes, A.Y. Chtchelkanova, D.M. and Treger, Spintronics: a spin-based electronics vision for the future., Science. 294 (2001) 1488–95.

[2] Z. Zhang, S. Satpathy, Electron states, magnetism, and the Verwey transition in magnetite, Phys. Rev. B. 44 (1991) 13319–13331. doi:10.1103/PhysRevB.44.13319.

[3] K.S. Yoon, J.H. Koo, Y.H. Do, K.W. Kim, C.O. Kim, J.P. Hong, Performance of $Fe_3O_4/AlO_x/CoFe$ magnetic tunnel junctions based on half-metallic Fe_3O_4 electrodes, J. Magn. Magn. Mater. 285 (2005) 125–129. doi:10.1016/j.jmmm.2004.07.025.

[4] P.J. van der Zaag, P.J.H. Bloemen, J.M. Gaines, R.M. Wolf, P.A.A. van der Heijden, R.J.M. van de Veerdonk, W.J.M. de Jonge, On the construction of an Fe_3O_4-based all-oxide spin valve, J. Magn. Magn. Mater. 211 (2000) 301–308. doi:10.1016/S0304-8853(99)00751-9.

[5] C. Park, Jian-Gang Zhu, Yingguo Peng, D.E. Laughlin, R.M. White, Inverse magnetoresistance in magnetic tunnel junction with an Fe_3O_4 electrode, IEEE Trans. Magn. 41 (2005) 2691–2693. doi:10.1109/TMAG.2005.855294.

[6] A. Kumar, S. Chaudhary, D.K. Pandya, S.K. Sharma, Evidence of electron-phonon and spin-phonon couplings at the Verwey transition in Fe_3O_4, Phys. Rev. B. 90 (2014) 24302. doi:10.1103/PhysRevB.90.024302.

[7] S. Tiwari, D.M. Phase, R.J. Choudhary, Probing antiphase boundaries in Fe_3O_4 thin films using micro-Raman spectroscopy, Appl. Phys. Lett. 93 (2008) 234108. doi:10.1063/1.3046788.

[8] E. J. W. VERWEY, Electronic Conduction of Magnetite (Fe_3O_4) and its Transition Point at Low Temperatures, Nature. 144 (1939) 327–328. doi:10.1038/144327b0.

[9] A. Kumar, D.K. Pandya, S. Chaudhary, Structural,electronic,and magnetic behavior of two dimensional epitaxial Fe_3O_4/TiN/Si(100) system, Appl. Phys. Lett. 102 (2013) 152406. doi:10.1063/1.4802235.

[10] A. Kumar, D.K. Pandya, S. Chaudhary, Reduction in anti-ferromagnetic interactions in ion-beam deposited Fe_3O_4 thin films, J. Appl. Phys. 111 (2012) 73901. doi:10.1063/1.3699309.

[11] X.H. Liu, A.D. Rata, C.F. Chang, A.C. Komarek, L.H. Tjeng, Verwey transition in Fe_3O_4 thin films : Influence of oxygen stoichiometry and substrate-induced microstructure, Phys. Rev. B. 90 (2014) 125142. doi:: 10.1103/PhysRevB.90.125142.

[12] D.T. Margulies, F.T. Parker, F.E. Spada, R.S. Goldman, J. Li, R. Sinclair, A.E. Berkowitz, Anomalous moment and anisotropy behavior in Fe_3O_4 films, Phys. Rev. B. 53 (1996) 9175–9187. doi:10.1103/PhysRevB.53.9175.

[13] F.C. Voogt, T.T.M. Palstra, L. Niesen, O.C. Rogojanu, M.A. James, T. Hibma, Superparamagnetic behavior of structural domains in epitaxial ultrathin magnetite films, Phys. Rev. B. 57 (1998) R8107–R8110. doi:10.1103/PhysRevB.57.R8107.

[14] S. Jain, A.O. Adeyeye, D.Y. Dai, Magnetic properties of half-metallic Fe_3O_4 films, J.

Appl. Phys. 95 (2004) 7237. doi:10.1063/1.1651800.

[15] S.K. Arora, R.G.S. Sofin, I. V. Shvets, Magnetoresistance enhancement in epitaxial magnetite films grown on vicinal substrates, Phys. Rev. B. 72 (2005) 134404. doi:10.1103/PhysRevB.72.134404.

[16] A. Kumar, D.K. Pandya, S. Chaudhary, Electric field assisted sputtering of Fe_3O_4 thin films and reduction in anti-phase boundaries, J. Appl. Phys. 112 (2012) 73909. doi:10.1063/1.4757012.

[17] B. Mauvernay, L. Presmanes, S. Capdeville, V.G. de Resende, E. De Grave, C. Bonningue, P. Tailhades, Elaboration and characterization of $Fe_{1-x}O$ thin films sputter deposited from magnetite target, Thin Solid Films. 515 (2007) 6532–6536. doi:10.1016/j.tsf.2006.11.131.

[18] S. Husain, F. Rahman, N. Ali, P.A. Alvi, Nickel Sub-lattice Effects on the Optical Properties of ZnO Nanocrystals, J. Optoelectron. Eng. 1 (2013) 28–32. doi:10.12691/joe-1-1-5.

[19] Y. Liu, Y. Wang, S. Zhou, S. Lou, L. Yuan, T. Gao, X. Wu, X. Shi, K. Wang, Synthesis of High Saturation Magnetization Superparamagnetic Fe_3O_4 Hollow Microspheres for Swift Chromium Removal, ACS Appl. Mater. Interfaces. 4 (2012) 4913–4920. doi:10.1021/am301239u.

[20] M. Baghaie Yazdi, K.Y. Choi, D. Wulferding, P. Lemmens, L. Alff, Raman study of the Verwey transition in magnetite thin films, New J. Phys. 15 (2013) 103032. doi:10.1088/1367-2630/15/10/103032.

[21] R.S. Hassan, T. Gaudisson, N. Yaacoub, J.M. Grenèche, N. Menguy, N. Nedelko, A. Slawska-Waniewska, M. Galmiche, F. Mammeri, S. Ammar, Granular $Fe_{3-x}O_4CoO$ hetero-nanostructures produced by in situ seed mediated growth in polyol: magnetic

properties and chemical stability, Mater. Res. Express. 1 (2014) 25035. doi:10.1088/2053-1591/1/2/025035.

[22] J.-B. Moussy, S. Gota, A. Bataille, M.-J. Guittet, M. Gautier-Soyer, F. Delille, B. Dieny, F. Ott, T. Doan, P. Warin, P. Bayle-Guillemaud, C. Gatel, E. Snoeck, Thickness dependence of anomalous magnetic behavior in epitaxial Fe_3O_4(111) thin films: Effect of density of antiphase boundaries, Phys. Rev. B. 70 (2004) 174448. doi:10.1103/PhysRevB.70.174448.

[23] J.P. Wright, J.P. Attfield, P.G. Radaelli, Long Range Charge Ordering in Magnetite Below the Verwey Transition, Phys. Rev. Lett. 87 (2001) 266401. doi:10.1103/PhysRevLett.87.266401.

[24] O. Chichvarina, T.S. Herng, W. Xiao, X. Hong, J. Ding, Magnetic anisotropy modulation of epitaxial Fe_3O_4 films on MgO substrates, J. Appl. Phys. 117 (2015) 17D722. doi:10.1063/1.4918695.

[25] M. Bohra, K.E. Prasad, R. Bollina, S.C. Sahoo, N. Kumar, Characterizing the phase purity of nanocrystalline Fe_3O_4 thin films using Verwey transition, J. Magn. Magn. Mater. 418 (2016) 137–142. doi:10.1016/j.jmmm.2016.02.010.

Table 1. The calculated values of line shape parameters and electron phonon coupling constant (λ) of A_{1g} and T_{2g} (3) vibrational mode.

	A_{1g}			T_{2g}		
Sample	ω (cm^{-1})	Γ (cm^{-1})	λ	ω (cm^{-1})	Γ (cm^{-1})	λ
F2.2	664.94	38.06	0.111	304.75	34.10	0.472
F2.5	665.31	37.47	0.114	302.70	32.57	0.457
F2.8	664.78	39.49	0.116	303.35	32.37	0.452
F3.0	666.53	38.73	0.111	302.59	42.20	0.592

Figure Captions:

Fig. 1 XRD patterns of Fe_3O_4 thin films grown at various P_{O_2} range from 2.2 to 3.0×10^{-5} Torr at 500°C substrate temperature.

Fig. 2 Raman spectra recorded at room temperature on the samples grown (a) at various substrate temperatures (400°C-600°C) in the environment of fixed P_{O_2} (3×10^{-5} Torr) and (b) at various P_{O_2} on the optimum substrate temperature (500°C).

Fig. 3 Raman spectra recorded at room temperature and their fits with the symmetric-antisymmetric Lorentzian curves for (a) A_{1g} and (b) T_{2g} (3) modes for all samples.

Fig. 4 In-plane magnetization hysteresis loops measured at room temperature on the samples grown at various P_{O_2}.

Fig. 5 Thermo-magnetization curves recorded in zero field and field cooled (H_a =200Oe) warming for (a) F2.2, (b) F2.5, (c) F2.8, and (d) F3.0 samples.

Fig. 6 The dM/dT plots for (a) F2.2, (b) F2.5, (c) F2.8, and (d) F3.0 samples. The Verwey transition (Tv) and isotropic temperature (T_k) for all the samples are noted therein.

Fig. 7 Resistivity vs. temperature plots for (a) F2.2, (b) F2.5, (c) F2.8, and (d) F3.0 samples.

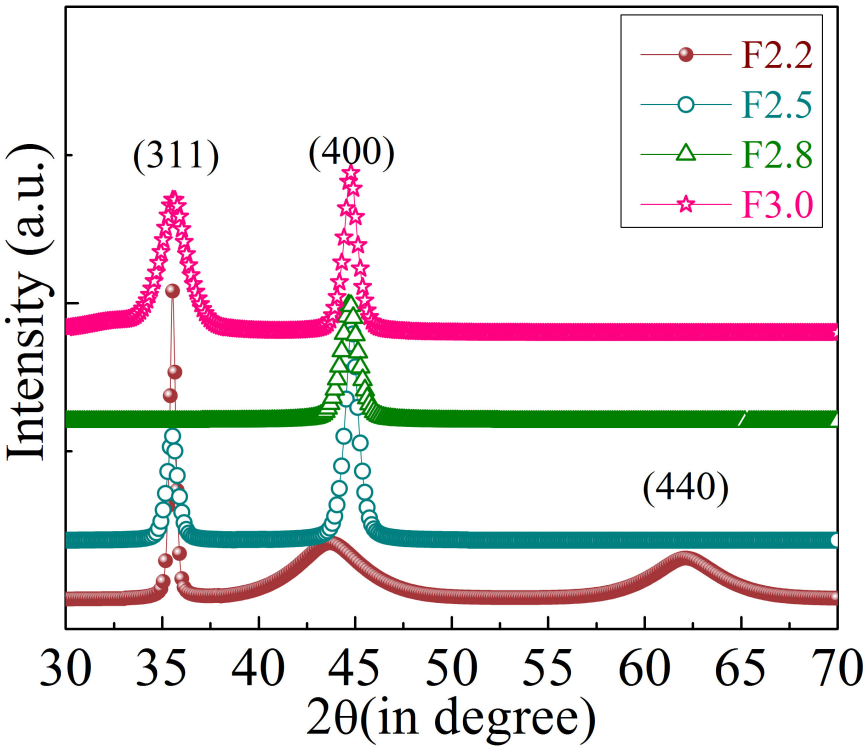

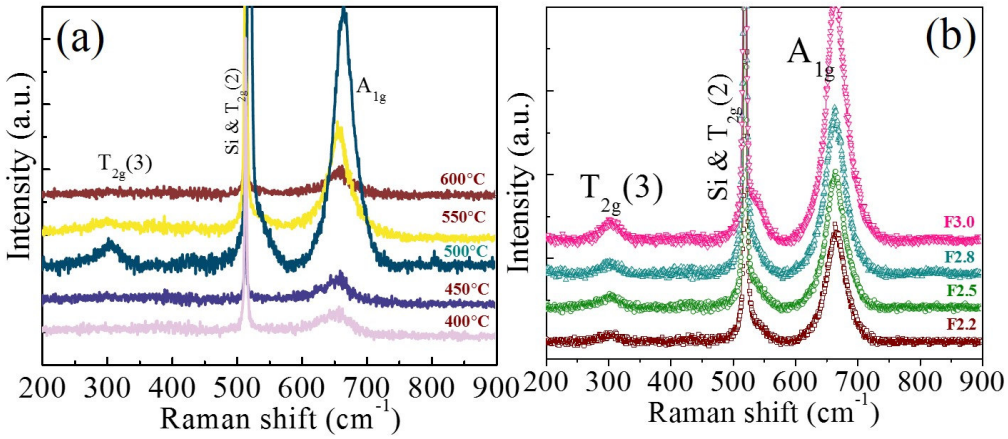

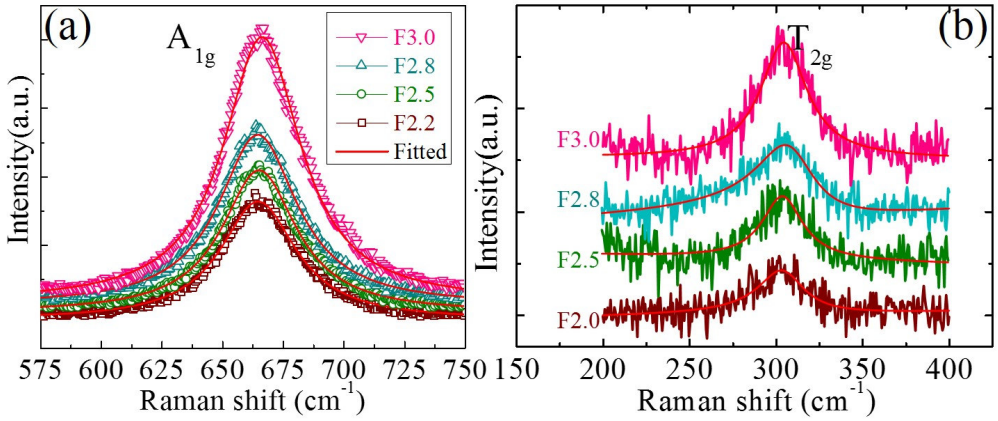

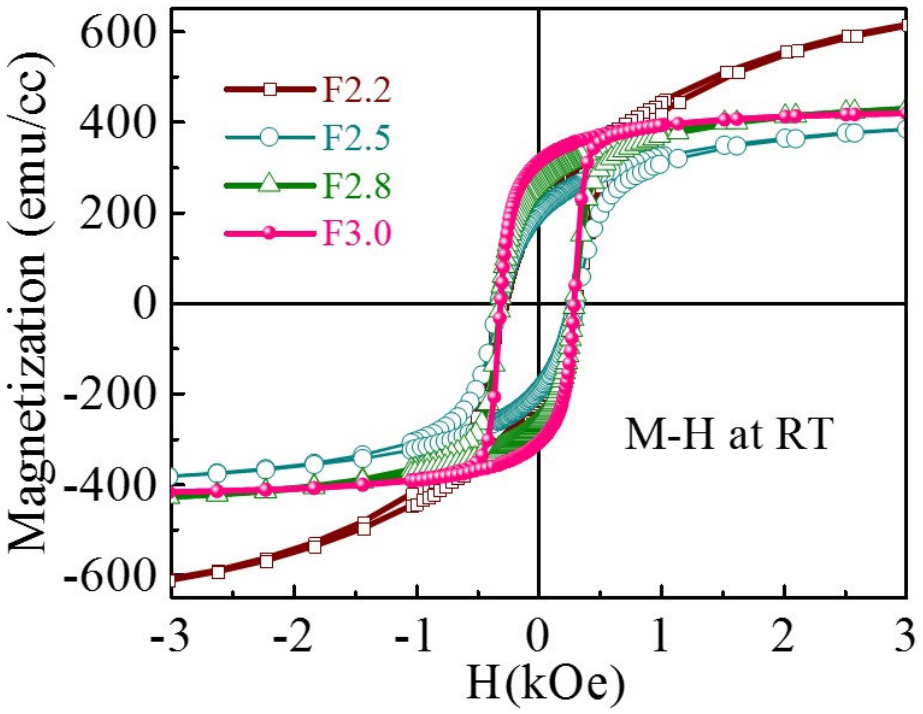

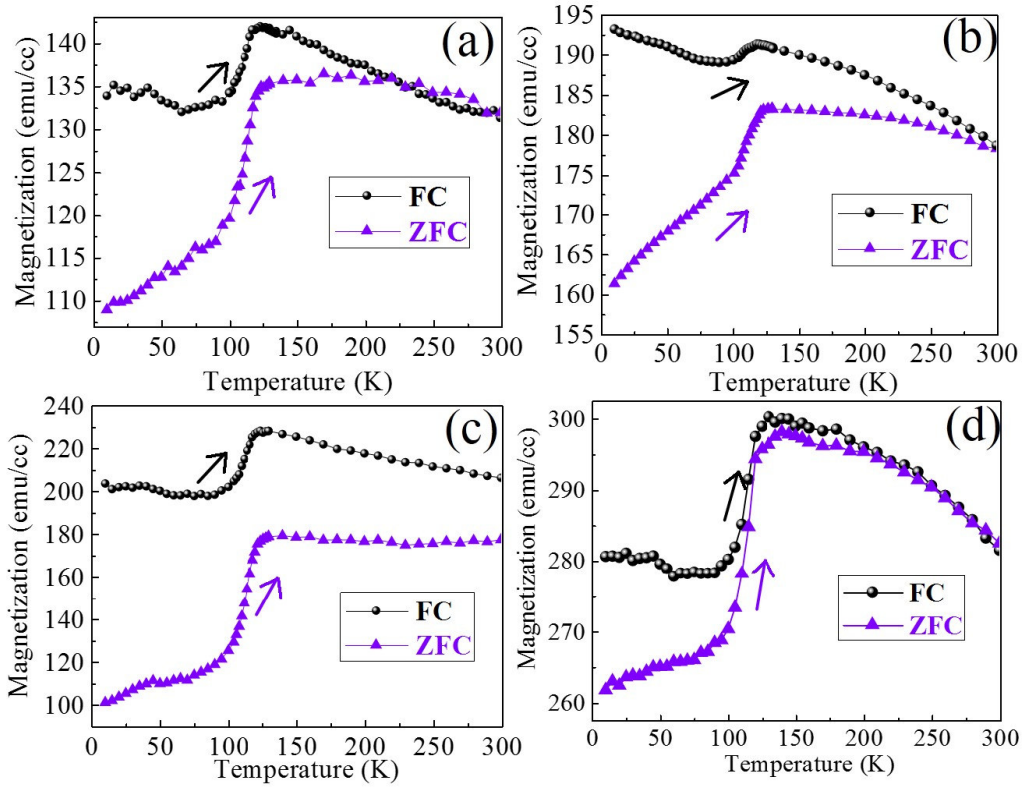

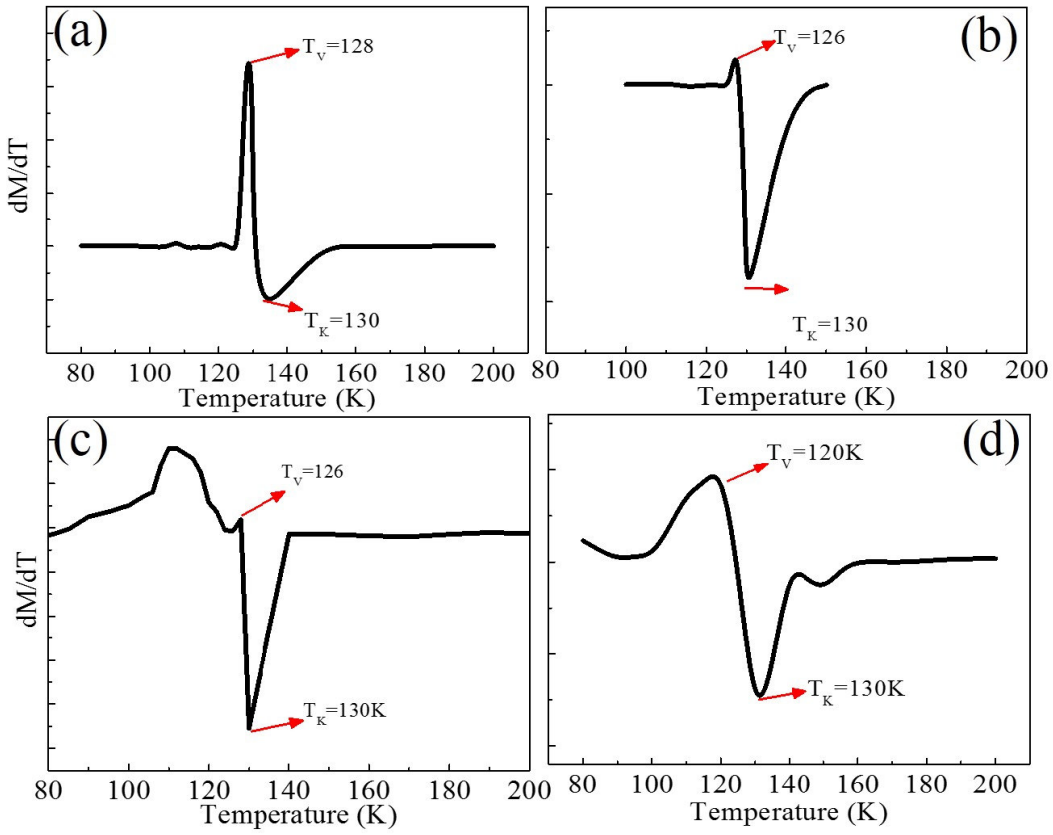

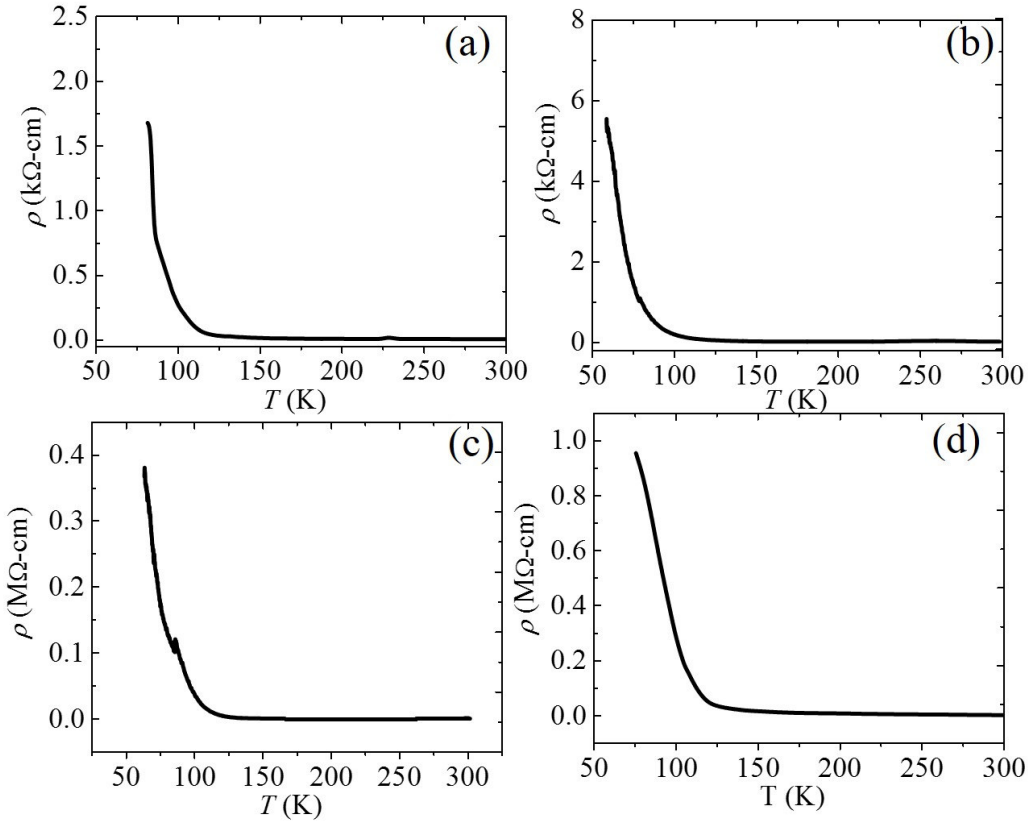

Highlights

- Fe_3O_4 thin films grown at various P_{O_2} on Si(100) by DC magnetron sputtering.
- APBs has been probed using Raman, magnetization and electron-transport measurements.
- Sharp Tv and low e-p coupling constant observed for higher P_{O_2} grown thin film.